PHYSICAL REVIEW B VOLUME 18, NUMBER 2 15 JULY 1978

Interaction between local phonon modes and plasmons in n-type semiconductors

R. Sirko, K. R. Subbaswamy, and D. L. Mills
Department of Physics, University of California, Irvine, California 92717
(Received 24 March 1978)

We present a theory of the interaction between plasmons and electric-dipole-active local phonon modes in an n-type semiconductor, when the impurities that produce the local phonon modes are present at finite concentration. Our theory is based on the observation that the equations satisfied by the relevant response functions are, within the random-phase approximation, close in form to a well-known model of a random alloy. A simple form of the coherent-potential approximation may then be used to explore the dynamical response of the plasmon–local-mode system. We explore a number of features of the response and illustrate how particular aspects may be probed through light-scattering studies.

I. INTRODUCTION

The interaction between electron plasma oscillations in n-type semiconductors and long-wavelength optical phonons has been the topic of considerable theoretical and experimental study.[1] One finds strong coupling between the plasmon and the longitudinal-optical phonon in polar materials, since the LO phonon sets up a macroscopic electric field.

Some years ago, Maradudin and Sham[2] inquired if a similar strong interaction results between an electric-dipole-active local phonon mode of frequency ω_0, and electron-plasma oscillations with frequency ω_p adjusted near ω_0 by appropriate doping of a semiconducting material. Through examination of the interaction between an isolated impurity and the electron plasma, they concluded the interaction was extraordinarily weak, with little chance of experimental detection.

It is not hard to appreciate the physical reason that led to this conclusion. As the (electric-dipole-active) local mode is excited, an oscillating electric field drives the electron plasma in the near vicinity of the impurity. The disturbance in the electron gas is not localized near the impurity, but has a radius equal to the Thomas-Fermi screening length, which is large compared to a lattice constant in typical semiconductors. Most of the oscillating charge density associated with the "local plasmon" thus lies far from the impurity where the oscillating electric field set up by its motion is very weak. Even though ω_p and ω_0 may differ only slightly, the interaction between the two excitations is thus very weak.

On the other hand, in reflectivity studies of n-type GaAs doped with small concentrations of phosphorous, Spitzer finds strong coupling between the plasmon and the local modes associated with the phosphorous impurity.[3] This has prompted us to reexamine the question raised by Maradudin and Sham.

While we believe the Maradudin-Sham calculation to be correct in all essential features, qualitatively new features enter when the impurities are present with finite concentration, even though this concentration is small. One may then have long-wavelength collective excitations of the impurity array which generate a macroscopic electric field. This macroscopic electric field may couple to the plasmon in the same manner as that associated with an LO phonon in a pure matrix.

The long-wavelength collective excitations of the local-mode–electron-plasma system mentioned in the preceding paragraph may be described readily by replacing the disordered array of impurities by an averaged uniform distribution of oscillator strength, in a spirit similar to the "virtual crystal" approximation employed in the theory of alloys.[4] Such an approach has proved simple and useful in theories of the collective motion of impurities, in models of undoped materials.[5,6] If applied to the present problem, however, this procedure has the disadvantage that it does not reproduce the results of Maradudin and Sham, in the one-impurity limit.

In the present paper, we present a theory of the coupling between electric-dipole-active local phonon modes and plasmons which incorporates the collective modes present at long wavelength and finite concentration, but which reproduces results equivalent to those of Maradudin and Sham in the one-impurity limit.[7] We find that in experiments which probe the long-wavelength response of the system, the collective modes of the system can provide the dominant features one observes. We show this through theoretical analysis of the spectrum of light scattered inelastically from the system.

If the impurities are embedded in a lattice of zinc-blende material (an example is the $\mathrm{GaAs}_{1-x}P_x$ system), then we show that through light scattering experiments the selection rules allow one to probe either the collective response of the system, the local mode described by Maradudin and Sham, or have both simultaneously present in the same spectrum. Crudely speaking, while collective modes analogous to the L_+ and L_- modes in pure materials[1] dominate the long-wavelength response, at short wavelengths it is in essence the Maradudin-Sham mode one excites, i.e., an experiment which probes the *local* response in the near vicinity of the impurity sees not the collective modes (present in a limited volume of phase space near $\vec{k}=0$), but rather the local phonon mode shifted very slightly in frequency by coupling to the electron plasma, as described in Ref. (2). As pointed out in an earlier paper,[6] when one examines the scattering of light from a disordered system, as in neutron scattering, one finds both incoherent and coherent contributions to the cross section. The incoherent contributions to the cross section, which describe wave-vector nonconserving scatterings, allow the light to probe the short-wavelength response and hence the near vicinity of the impurity.

The outline of this paper is as follows. Section II sets up our basic model, and derives the equations satisfied by the basic response functions of the theory. We also explore special limits here, and then develop and explore an application of the coherent potential approximation to the problem. In Sec. III we turn to a discussion of Raman scattering from the excitations of the plasmon-impurity-local-mode system.

II. MODEL AND RESPONSE FUNCTIONS OF THE SYSTEM

We consider a host lattice, later presumed to have the zinc-blende structure, within which a small concentration of ionic impurities is distributed on one sublattice. The impurities occupy equivalent sites, and have mass substantially smaller than the host ions they replace. They thus give rise to phonon modes with frequency higher than that characteristic of the host-lattice phonons. The displacement field of these modes, which has frequency ω_0, is localized very near a given impurity.

The material is doped with electrons that move in a parabolic conduction band of mass m^*, and our interest is in carrier concentrations where the plasma frequency $\omega_p=(4\pi ne^2/m^*\epsilon_\infty)^{1/2}$ is comparable to ω_0. Here n is the carrier concentration, and ϵ_∞ the dielectric constant characteristic of frequencies high compared to host-lattice frequencies, but well below the band gap.

We write the Hamiltonian of our system in the form

$$H=H_I+H_e+H_{Ie}+H_{ee}\,, \tag{1}$$

where H_I and H_e describe the noninteracting impurity local modes and noninteracting conduction electrons, respectively. The last two terms describe the local-mode–conduction-electron interaction and the electron-electron interaction, respectively.

We ignore the lattice vibrations of the host lattice in the present discussion, under the presumption that the frequencies of interest here are high compared to the frequencies of the host matrix. Since the impurity local modes will be presumed infrared active, with an electric dipole moment proportional to the displacement $\vec{u}$ of the impurity, a complete description will include the dipole-dipole interaction between impurities. We ignore this coupling here, and we point out the consequences of this oversight as we proceed. At low impurity concentrations, the influence of the dipolar coupling between impurities will have no quantitative effect on our results.

The terms H_I and H_e in Eq. (1) are written

$$H_I=\omega_0\sum_{1}\sum_{\mu=1}^{3}c(\vec{l})a^\dagger_{\vec{l}\mu}a_{\vec{l}\mu} \tag{2}$$

and

$$H_e=\sum_{\vec{k}}\frac{k^2}{2m^*}c^\dagger_{\vec{k}}c_{\vec{k}}\equiv\sum_{\vec{k}}\epsilon(\vec{k})c^\dagger_{\vec{k}}c_{\vec{k}}\,. \tag{3}$$

In Eq. (2) $a_{\vec{l}\mu}$ $(a^\dagger_{\vec{l}\mu})$ is the boson annihilation (creation) operator associated with the local mode on lattice site $\vec{l}$. The local mode is threefold degenerate, with μ a polarization index. The sum on $\vec{l}$ ranges over all sites of the sublattice, and $c(\vec{l})$ is unity if a given site is occupied by an impurity and zero otherwise. Thus, if by $\langle c(\vec{l})\rangle$ we mean the average of $c(\vec{l})$ over all sites on the sublattice, we have $\langle c(\vec{l})\rangle=\langle c(\vec{l})^2\rangle=c$, where c is the impurity concentration. We work in units with $\hbar=1$.

In Eq. (3), $c_{\vec{k}}$ and $c^\dagger_{\vec{k}}$ are the electron creation and annihilation operators. We ignore explicit reference to spin, but include the relevant factors of two later.

The electron-electron interaction H_{ee} is given by

$$H_{ee}=\frac{1}{2}\sum_{\vec{k}\vec{k}'\vec{q}}V_c(\vec{q})c^\dagger_{\vec{k}+\vec{q}}c^\dagger_{\vec{k}'-\vec{q}}c_{\vec{k}'}c_{\vec{k}}\,, \tag{4}$$

where $V_c(\vec{q})=4\pi e^2/\epsilon_\infty q^2$. We have assumed a unit volume.

If e^* is the dipole-moment effective charge of the impurity ions, then H_{Ie} may be written

$$H_{Ie}=-e^*\sum_{\vec{l}\mu}c(\vec{l})u_\mu(\vec{l})E_\mu(\vec{l})\,, \tag{5}$$

where $u_\mu(\vec{l})$ is the μth Cartesian component of the local-mode displacement, which can be written

$$u_\mu(\vec{l})=(1/2M_I\omega_0)^{1/2}(a_{\vec{l}\mu}+a^\dagger_{\vec{l}\mu})\,, \tag{6}$$

with M_I the reduced mass of the impurity. The electric field $E_\mu(\vec{l})$ is that set up by a density fluctuation in the electron gas. In terms of the operator $\psi(\vec{x})=\sum_{\vec{k}} c_{\vec{k}} \exp(i\vec{k}\cdot\vec{x})$ we have

$$E_\mu(\vec{R})=-\frac{e}{\epsilon_\infty}\frac{\partial}{\partial R_\mu}\int d^3x\,\frac{\psi^\dagger(\vec{x})\psi(\vec{x})}{|\vec{x}-\vec{R}|}\,. \tag{7}$$

The results above combine to give

$$H_{Ie}=i\gamma_0\sum_{\vec{l}\mu}\sum_{\vec{k}\vec{q}} c(\vec{l})(a_{\vec{l}\mu}+a^\dagger_{\vec{l}\mu})\frac{q_\mu}{q^2}c^\dagger_{\vec{k}+\vec{q}}c_{\vec{k}} \times\exp(-i\vec{q}\cdot\vec{l})\,, \tag{8}$$

with the coupling constant $\gamma_0=(4\pi ee^*/\epsilon_\infty)\times(1/2M_I\omega_0)^{1/2}$.

To examine the dynamical properties of our system, we use the temperature Green's-function formalism, which through its extension to real time Green's functions allows us to examine the linear response of the system to an external probe. Since this formalism is by now standard,[8] we only sketch the derivation of the Dyson equations that form the basis of the present analysis. However, it proves useful to set down the definitions of the Green's functions we analyze.

A fundamental Green's function is the electron density fluctuation propagator defined by

$$\chi(\vec{x}\tau,\vec{x}'\tau')=-\langle T_\tau[\delta n(\vec{x}\tau)\delta n(\vec{x}'\tau')]\rangle\,. \tag{9}$$

Here τ is an imaginary time, T_τ the Wick time-ordering operator, $\delta n(\vec{x}\tau)=\exp(H\tau)\delta n(\vec{x})\exp(-H\tau)$, with $\delta n(\vec{x})$ the density fluctuation operator

$$\delta n(\vec{x})=\psi^\dagger(\vec{x})\psi(\vec{x})-\langle\psi^\dagger(\vec{x})\psi(\vec{x})\rangle\,. \tag{10}$$

We also have an impurity local-mode propagator which we write

$$D(\vec{l}\,\mu\tau,\vec{l}'\mu'\tau')=\langle T_\tau[\varphi_{\vec{l}\mu}(\tau)\varphi_{\vec{l}'\mu'}(\tau')]\rangle c(\vec{l})c(\vec{l}')\,, \tag{11}$$

with $\varphi_{\vec{l}\mu}(\tau)=\exp(H\tau)\varphi_{\vec{l}\mu}\exp(-H\tau)$ and $\varphi_{\vec{l}\mu}=a_{\vec{l}\mu}+a^\dagger_{\vec{l}\mu}$.

In the absence of both electron-electron interactions and the electron impurity interaction, simple standard forms obtain for both propagators defined above. For the density fluctuation propagator, in this limit

$$\chi(\vec{x}\tau,\vec{x}'\tau')=\frac{1}{\beta}\sum_{\vec{k},i\omega_m} e^{i\vec{k}\cdot(\vec{x}-\vec{x}')}e^{-i\omega_m(\tau-\tau')}\chi_0(\vec{k},i\omega_m)\,, \tag{12}$$

where $\beta=(k_BT)^{-1}$ with k_B Boltzmann's constant and T the absolute temperature, and $\omega_m=2\pi m/\omega$. In Eq. (12),

$$\chi_0(\vec{k},i\omega_m)=\frac{2}{\beta}\sum_{\vec{q},i\omega_n}G_0(\vec{q},i\omega_n)G_0(\vec{q}+\vec{k},i\omega_n+i\omega_m)\,, \tag{13}$$

where $G_0(\vec{q},i\omega_n)=[i\omega_n-\epsilon(\vec{q})]^{-1}$ and $\omega_n=\pi(2n+1)/\beta$.

For the impurity-local-mode propagator, in the absence of coupling between the impurities and the electrons we have, noting that $c^2(\vec{l})=c(\vec{l})$,

$$D(\vec{l}\mu\tau,\vec{l}'\mu'\tau')=c(\vec{l})\delta_{\vec{l}\vec{l}'}\delta_{\mu\mu'}\frac{1}{\beta}\times\sum_{i\omega_m}e^{-i\omega_m(\tau-\tau')}D_0(i\omega_m)\,, \tag{14}$$

where again $\omega_m=2\pi m/\beta$ is the "boson frequency" of the imaginary time propagator formalism, and

$$D_0(i\omega_m)=\frac{2\omega_0}{\omega_0^2+\omega_m^2+2\omega_0\Pi(\omega_m)}\,, \tag{15}$$

where $\Pi(\omega_m)$ is the proper self-energy associated with the local-mode Green's function in the absence of coupling to electrons. The proper self-energy is presumed nonzero by virtue of anharmonic terms present in the phonon Hamiltonian of the disordered crystal. In the dilute limit, $\Pi(\omega_m)$ may be presumed independent of impurity concentration. We do not examine the structure of $\Pi(\omega_m)$ explicitly here, but acknowledge its presence to introduce the damping of the local mode produced by anharmonicity. In the end, when we continue $D_0(i\omega_m)$ off the imaginary to the real axis of the complex frequency plane, $2\omega_0\Pi(\omega_m)$ will be replaced by a phenomenological damping constant. Note that we presume here that $\Pi(\omega_m)$ is unaffected by the electron–local-mode coupling. We believe this quite a reasonable presumption.

In the presence of both H_{Ie} and H_{ee}, through use of diagrammatic methods, we next proceed to derive a set of Dyson equations satisfied by the two basic propagators introduced above. To do this, it is useful to introduce the Fourier transform $\chi(\vec{\kappa}\vec{\kappa}';i\omega_m)$ of $\chi(\vec{x},\vec{x}';i\omega_m)$ defined by

$$\chi(\vec{x},\vec{x}';i\omega_m)=\sum_{\vec{\kappa}\vec{\kappa}'}e^{i\vec{\kappa}\cdot\vec{x}-i\vec{\kappa}'\cdot\vec{x}'}\chi(\vec{\kappa},\vec{\kappa}';i\omega_m)\,. \tag{16}$$

We first set down the Dyson equation satisfied by $\chi(\vec{\kappa}\vec{\kappa}';i\omega_n)$ for the case where the electron-electron interaction H_{ee} may be set to zero. The Dyson equation is illustrated in Fig. 1 [within the framework of a random-phase approximation (RPA) description], and becomes

$$\chi(\vec{\kappa}\vec{\kappa}';i\omega_m)=\chi_0(\vec{\kappa};i\omega_m)\delta_{\vec{\kappa}\vec{\kappa}'}-\gamma_0^2D_0(i\omega_m)\chi_0(\vec{\kappa};i\omega_m)\times\sum_{\vec{l}\mu}\sum_{\vec{\kappa}''}c(\vec{l})\frac{\kappa_\mu\kappa''_\mu}{\kappa^2\kappa''^2}\exp(i\vec{\kappa}''\cdot\vec{l}-i\vec{\kappa}\cdot\vec{l})\times\chi(\vec{\kappa}''\vec{\kappa}';i\omega_m)\,. \tag{17}$$

If electron-electron interactions are included (again in the RPA), Eq. (17) is left unchanged in structure, except that the free density fluctuation propagator $\chi_0(\vec{\kappa},i\omega_m)$ is replaced by $\chi^{(p)}(\vec{\kappa},i\omega_m)$

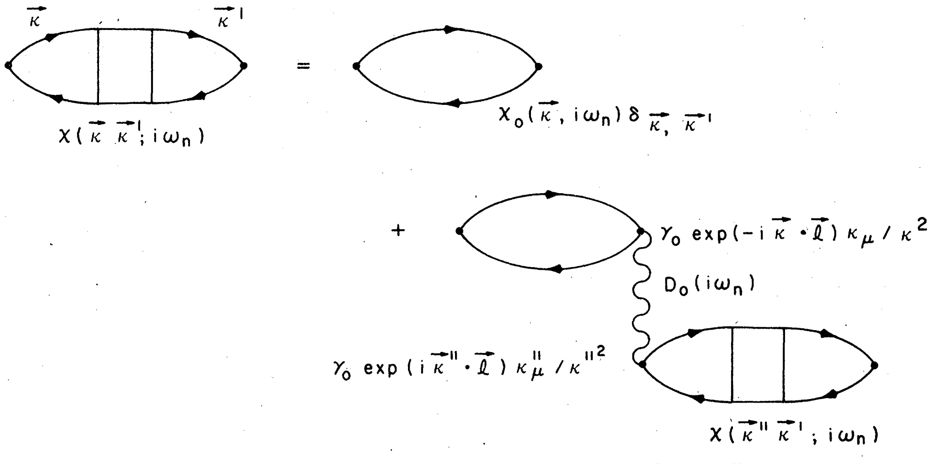

FIG. 1. Illustration of the Dyson equation satisfied by the electron density fluctuation propagator.

$=\chi_0(\vec{\kappa},i\omega_m)/[1-V_c(\vec{\kappa})\chi_0(\vec{\kappa},i\omega_m)]$. In what follows, we presume this replacement has been made everywhere.

Again within the RPA, the Dyson equation for $D(\vec{l}\mu,\vec{l}'\mu';i\omega_m)$ may be written

$$D(\vec{l}\mu,\vec{l}'\mu';i\omega_m)=c(\vec{l})\delta_{\vec{l}\vec{l}'}\delta_{\mu\mu'}D_0(i\omega_m)-\gamma_0^2D_0(i\omega_m)\times\sum_{\vec{\kappa}}\sum_{\vec{l}''\mu''}c(\vec{l}'')\frac{\kappa_\mu\kappa_\mu}{\kappa^4}\chi^{(p)}(\vec{\kappa},i\omega_m)\times\exp[i\vec{\kappa}\cdot(\vec{l}-\vec{l}'')]\times D(\vec{l}''\mu'',\vec{l}'\mu';i\omega_m)\,. \tag{18}$$

Our principal task is to develop approximate solutions to the equations derived above, with attention to the physical considerations of Sec. I.

It is useful to begin by multiplying Eq. (17) by $\exp(i\vec{\kappa}\cdot\vec{l}-i\vec{\kappa}'\cdot\vec{l}')$, then sum on $\vec{\kappa}$ and $\vec{\kappa}'$ to form an equation for $\chi(\vec{x}\vec{x}';i\omega_m)$. One has, with

$$\chi^{(p)}(\vec{l}-\vec{l}';i\omega_m)=\sum_{\vec{\kappa}}\chi^{(p)}(\vec{\kappa};i\omega_m)\exp[i\vec{\kappa}\cdot(\vec{l}-\vec{l}')]\,, \tag{18a}$$

$$\chi_\mu^{(p)}(\vec{l}-\vec{l}';i\omega_m)=\sum_{\kappa}\frac{\kappa_\mu}{\kappa^2}\chi^{(p)}(\vec{\kappa},i\omega_m)\exp[i\vec{\kappa}\cdot(\vec{l}-\vec{l}')]\,, \tag{18b}$$

and

$$\chi_\mu(\vec{l},\vec{l}';i\omega_m)=\sum_{\vec{\kappa}\vec{\kappa}'}\frac{\kappa_\mu}{\kappa^2}\chi(\vec{\kappa}\vec{\kappa}';i\omega_m)\times\exp(i\vec{\kappa}\cdot\vec{l}-i\vec{\kappa}'\cdot\vec{l}')\,, \tag{18c}$$

the relation

$$\chi(\vec{l}\vec{l}';i\omega_m)=\chi^{(p)}(\vec{l}-\vec{l}',i\omega_m)-\gamma_0^2D_0(i\omega_m)\sum_{\vec{l}''\mu}c(\vec{l}'')\chi_\mu^{(p)}(\vec{l}-\vec{l}'';i\omega_m)\times\chi_\mu(\vec{l}'',\vec{l}';\omega_m)\,. \tag{19}$$

We thus encounter a new propagator $\chi_\mu(\vec{l}\vec{l}';\omega_m)$. From Eq. (17) a closed equation for this function is generated, through use of the same procedure used to obtain Eq. (19). We have

$$\chi_\mu(\vec{l}\vec{l}';i\omega_m)=\chi_\mu^{(p)}(\vec{l}-\vec{l}';i\omega_m)-\gamma_0^2D_0(i\omega_m)\times\sum_{\vec{l}''\mu'}c(\vec{l}'')\chi_{\mu\mu'}^{(p)}(\vec{l}-\vec{l}'';i\omega_m)\times\chi_{\mu'}(\vec{l}'',\vec{l}';i\omega_m)\,, \tag{20}$$

where we introduce, in analogy with Eq. (18b),

$$\chi_{\mu\mu'}^{(p)}(\vec{l}-\vec{l}';i\omega_m)=\sum_{\vec{\kappa}}\frac{\kappa_\mu\kappa_{\mu'}}{\kappa^4}\chi^{(p)}(\vec{\kappa},i\omega_m)\times\exp[i\vec{\kappa}\cdot(\vec{l}-\vec{l}')]\,. \tag{21}$$

It is the approximate solution of Eq. (20) that will concern us later. Note that Eq. (18) is readily cast into a form very similar in structure to Eq. (20):

$$D(\vec{l}\mu,\vec{l}'\mu';i\omega_m)=\delta_{\vec{l}\vec{l}'}\delta_{\mu\mu'}D_0(i\omega_m)c(\vec{l})-\gamma_0^2D_0(i\omega_m)\times\sum_{\vec{l}''\mu''}c(\vec{l}'')\chi_{\mu\mu''}^{(p)}(\vec{l}-\vec{l}'';i\omega_m)\times D(\vec{l}''\mu''\vec{l}'\mu';i\omega_m)\,. \tag{22}$$

The only difference between the structure of Eq. (22) and that of Eq. (20) is the form of the inhomogeneous term.

If for the moment, we ignore the technical complication introduced by the Cartesian subscript μ in Eq. (21) or (22), then these equations have a structure identical to those encountered in the analysis of a simple model in the theory of random alloys.[9] This is the equation satisfied by the one-electron Green's function in the tight-binding description of a binary alloy, with one orbital on each site and "diagonal disorder" (i.e., all transfer integrals are assumed identical, and only the energy of each orbital varies from site to site). This model has been extensively studied, and the coherent-potential approximation (CPA) appears to describe its one electron properties well.[10] Thus, since our equations are isomorphic to those which describe a binary alloy with three orbitals per site and "diagonal disorder,"[11] we shall analyze Eqs. (21) and (22) within the coherent potential approximation. Before we do this, we examine the solution of Eqs. (21) and (22) in two simple limits.

A. Single-impurity limit

If only a single isolated impurity is present, then Eq. (18), and Eq. (19) in combination with Eq. (20), may be solved in closed form. The solution is easily obtained after noting that as $\vec{x} \to 0$, $\tilde{\chi}_{\mu\mu'}(\vec{x}, i\omega_m)$ becomes diagonal in μ and μ', with the diagonal elements independent of μ. After presuming the single impurity is located at the origin, we find from Eq. (18):

$$D(\vec{l}\mu, \vec{l}'\mu'; i\omega_m) = \frac{\delta_{\vec{l}0}\delta_{\vec{l}'0}\delta_{\mu\mu'}D_0(i\omega_m)}{1+\gamma_0^2 D_0(i\omega_m)\chi_{\mu\mu}^{(p)}(0, i\omega_m)}, \tag{23}$$

while Eq. (20) in combination with Eq. (19) gives for the density fluctuation propagator a form very similar to that encountered in a rather different context[12]:

$$\chi(\vec{x}, \vec{x}'; i\omega_m) = \chi^{(p)}(\vec{x}-\vec{x}'; i\omega_m) + \frac{\gamma_0^2 D_0(i\omega_m)}{1+\gamma_0^2 D_0(i\omega_m)\chi_{\mu\mu}^{(p)}(0, i\omega_m)} \times \sum_{\mu} \chi_{\mu}^{(p)}(\vec{x}, i\omega_m)\chi_{\mu}^{(p)}(\vec{x}', i\omega_m). \tag{24}$$

To obtain Eq. (24), we have noted that $\chi_{\mu}^{(p)}(\vec{x}, i\omega_m)$ is an odd function of the spatial coordinate $\vec{x}$.

The response functions displayed in Eq. (23) and (24) describe the dynamics of an isolated impurity coupled to the electron plasma. A comparison of Eq. (23) with Eq. (15) shows that in Eq. (23), the combination $-\gamma_0^2\chi_{\mu\mu}^{(p)}(0, i\omega_m)$ is the contribution to the (proper) self-energy of the local phonon mode from coupling to the electron plasma. When $D(\vec{l}\mu, \vec{l}'\mu'; i\omega_m)$ is analytically continued in the standard fashion to the near vicinity of the real axis in the frequency plane, the real part of $-\gamma_0^2\chi_{\mu\mu}^{(p)}(0, i\omega_m)$ describes a shift in the local-mode frequency from coupling to the electron plasma, while the imaginary part gives damping in addition to that provided by anharmonicity alone. In the presence of the electron plasma, the impurity motion is Landau damped by coupling to the particle-hole excitations in the electron gas.

It is straightforward to demonstrate that the frequency shift of the local mode produced by coupling including $-\gamma_0^2\chi_{\mu\mu}^{(p)}(0, i\omega_m)$ in the proper self energy is identical to the frequency shift calculated by Maradudin and Sham.[2] Their treatment of the frequency shift is equivalent to use of a rather schematic expression for $\chi_{\mu}^{(p)}(0, i\omega_m)$ in evaluating the proper self-energy contributed by the electron plasma. The present theory combined with a more realistic form for $\chi_{\mu}^{(p)}(0, i\omega_m)$ describes the Landau damping as well, and produces complete formulas for all of the response functions of the system.

For the physical reason discussed in Sec. I, Maradudin and Sham estimate the frequency shift from coupling to the electron plasma is unobservably small, since it is a small fraction of the shift produced by the anharmonicity always present. Thus, we do not explore the behavior of the isolated impurity in any quantitative fashion here, although the small contribution $-\gamma_0^2\chi_{\mu\mu}^{(p)}(0, i\omega_m)$ to the local-mode proper self-energy is included in the numerical work discussed in Sec. III.

B. Virtual-crystal approximation

In Sec. I we stressed that for finite concentration, the impurity-electron-plasma system possesses long-wavelength excitations of collective character. Quite clearly, no description of these collective modes can emerge from a theory which examines the response with only a single isolated impurity present. We turn to a simple approximate solution of the equations at finite concentration. This approximation procedure, which we call the virtual-crystal approximation following terminology employed elsewhere,[9] leads to a description of the collective motions of the system. However, in the limit of vanishing concentration, it fails to reproduce the one-impurity limit properly. We shortly turn to a more sophisticated scheme which produces both a description of the collective modes of the system and the one-impurity limit. That discussion will prove more comprehensible if we pause to examine the virtual-crystal approximation explicitly before proceeding to the full theory.

The virtual-crystal approximation is generated by replacing the factor $c(\vec{l})$ wherever it appears in Eqs. (18)–(20) by its average over all sites $\langle c(\vec{l})\rangle \equiv c$, with c the impurity concentration. Thus, the disordered crystal is replaced by a spatially homogeneous "virtual crystal," with the local-mode oscillator strength distributed over all sites in a manner that preserves its integrated strength.

Within the virtual crystal approximation, the response functions $\chi(\vec{x},\vec{x}';i\omega_m)$ and $D(\vec{l}\mu,\vec{l}'\mu';i\omega_m)$ become functions of the differences $\vec{x}-\vec{x}'$ and $\vec{l}-\vec{l}'$, respectively. We write

$$\chi(\vec{x},\vec{x}';i\omega_m)=\sum_{\vec{k}}\overline{\chi}(\vec{k},i\omega_m)e^{i\vec{k}\cdot(\vec{x}-\vec{x}')}\tag{25a}$$

and

$$D(\vec{l}\mu,\vec{l}'\mu';i\omega_m)=\sum_{\vec{k}}\overline{D}_{\mu\mu'}(\vec{k},i\omega_m)e^{i\vec{k}\cdot(\vec{l}-\vec{l}')},\tag{25b}$$

to find, with n_0 the number of unit cells per unit volume

$$\overline{\chi}(\vec{k},i\omega_m)=\frac{\chi^{(p)}(\vec{k},i\omega_m)}{1+cn_0\gamma_0^2k^{-2}D_0(i\omega_m)\chi^{(p)}(\vec{k},i\omega_m)},\tag{26a}$$

and

$$\overline{D}_{\mu\mu'}(\vec{k},i\omega_m)=\left(\delta_{\mu\mu'}-\frac{k_\mu k_{\mu'}}{k^2}\right)\overline{D}_t(\vec{k},i\omega_m)+\frac{k_\mu k_{\mu'}}{k^2}\overline{D}_l(\vec{k},i\omega_m)\tag{26b}$$

with

$$\overline{D}_l(\vec{k},i\omega_m)=\frac{D_0(i\omega_m)}{1+cn_0\gamma_0^2k^{-2}D_0(i\omega_m)\chi^{(p)}(\vec{k},i\omega_m)}\tag{27a}$$

and

$$\overline{D}_t(\vec{k},i\omega_m)\equiv D_0(i\omega_m).\tag{27b}$$

From Eqs. (26) and (27), we see that the impurity array has excitations of transverse character unshifted in frequency from the isolated local-mode frequency ω_0, while the longitudinal normal modes couple to the electron plasma. The frequencies of the longitudinal normal modes are found by replacing $i\omega_m$ by $\Omega+i\eta$, then seeking the zeros of the denominator in Eq. (27b) or equivalently in Eq. (26a). To explore the properties of these collective modes, the long-wavelength $\vec{k}\to 0$ is particularly simple. We have

$$\lim_{\vec{k}\to 0}\chi^{(p)}(\vec{k},i\omega_m)=\frac{nk^2}{m^*}\frac{1}{(i\omega_m)^2}\frac{1}{1+\omega_p^2/(i\omega_m)^2}.\tag{28}$$

Upon letting $i\omega_m\to\Omega+i\eta$, and replacing $2\omega_0\Pi(\Omega+i\eta)$ by a phenomenological damping constant $i\Omega\gamma$ with origin in anharmonicity, we find the frequency of the long-wavelength collective modes is found from

$$(\omega_0^2-\Omega^2-i\Omega\gamma)(\omega_p^2-\Omega^2)-c\Omega_p^2\omega_p^2=0,\tag{29}$$

where we introduce the ion plasma frequency $\Omega_p^2=4\pi n_0e^{*2}/M_I\epsilon_\infty$.

The roots that emerge from Eq. (29) describe coupled, collective motions of the local-mode–electron-plasma system that are the analog of the L_+ and L_- modes of the pure system.[1]

There is one simplification in our model Hamiltonian that introduces an error in Eq. (29) that for our purposes is quantitatively unimportant. If we had included dipolar coupling between the local modes associated with the impurities, then as in the treatment of Maradudin and Oitmaa[5] we would find that the *transverse* normal modes of the impurity array occur not at the frequency $\omega_t^2=\omega_0^2$ as found above, but rather at the frequency $\omega_t^2=\omega_0^2-\frac{1}{3}c\Omega_p^2$, where $\frac{1}{3}c\Omega_p^2$ is a downward shift from local fields of dipolar origin. Then in Eq. (27), we would find the frequency ω_0^2 replaced by a longitudinal frequency $\omega_l^2=\omega_t^2+c\Omega_p^2$. If we replace ω_0^2 in Eq. (27) by ω_l^2, then Eq. (29) may be rearranged to read

$$\epsilon_\infty+c\left[\Omega_p^2/(\omega_t^2-\Omega^2-i\Omega\gamma)\right]-\omega_p^2/\Omega^2=0.\tag{30}$$

Thus, the longitudinal normal modes are seen to occur at the zeros of the (spatially averaged) dielectric constant of the combined local-mode–electron-plasma system, as one would expect from elementary considerations.

The error introduced by the appearance of ω_0^2 rather than ω_l^2 in Eq. (29) is quantitatively negligible for our purposes, since the small shifts introduced by the factor $c\Omega_p^2$ for low concentrations are obscured by the effect of damping described phenomenologically by the factor $i\Omega\gamma$. Indeed, the Lyddane-Sachs-Teller splitting of the local-mode frequencies predicted by Maradudin and Oitmaa[5] has proved difficult to observe for precisely this reason.[13] We are presently extending the full description of the model and the discussion of Sec. III to mixed crystals where the minority constituent concentration is not small. For this extension, it is necessary to include the dipolar coupling fully.

At this point, we see that we have generated a set of equations for our system which properly yields the Maradudin and Sham description of the isolated impurity problem, while at finite concentrations a description of the collective excitations of the system emerges from the same equations. Our task is to build up a solution to the equations which incorporates both features.

As already remarked, the Dyson equations for the Green's functions, Eqs. (20) and (22) have a structure similar to the equation satisfied by the one electron Green's function in a random binary alloy.[9] Specifically, except for the Cartesian subscripts, our equations are identical in structure to that of the one-electron Green's function in the tight-binding description of a binary alloy with one orbital on each site and "diagonal disorder," i.e., all transfer integrals are assumed identical and only the energy of the orbital varies from site to site. This model has been extensively studied, and the CPA appears to describe its one-electron properties well. Since our equations are isomorphic to those which describe a binary alloy with three orbitals per site and "diagonal disorder," we analyze Eqs. (20) and (22) within the CPA. Since an extensive literature exists on this topic, our discussion of the CPA will be quite brief. In what follows we shall outline only the CPA calculation for $\chi_\nu(\vec{l}\,\vec{l}\,'; \omega)$ since the procedure for obtaining $D(\vec{l}\mu\vec{l}\,'\mu'; \omega)$ is identical.

We begin our CPA calculation by adding and subtracting an effective potential $\sigma(\omega)$ (yet to be determined) at each site $\vec{l}$ in Eq. (20), to get

$$\chi_\nu(\vec{l}\,\vec{l}\,'; \omega) = \chi_\nu(\vec{l} - \vec{l}\,'; \omega) + \sigma \sum_{\vec{l}''\mu} \chi^{(p)}_{\nu\mu}(\vec{l} - \vec{l}''; \omega)\, \chi_\mu(\vec{l}''\vec{l}\,'; \omega) + \sum_{\vec{l}''\mu} v_{\vec{l}''} \chi^{(p)}_{\nu\mu}(\vec{l} - \vec{l}''; \omega)\, \chi_\mu(\vec{l}''\vec{l}\,'; \omega), \tag{31}$$

where

$$v_{\vec{l}} = \begin{cases} v - \sigma \equiv v_I; & \vec{l} \text{ an impurity site} \\ -\sigma \equiv v_H; & \vec{l} \text{ a host site}, \end{cases} \tag{32}$$

and $v = -|\gamma_0|^2 D_0(\omega)$.

Expressing this equation in terms of the Fourier transforms of the quantities involved yields,

$$\chi_\nu(\vec{\kappa}\vec{\kappa}\,'; \omega) = \chi_\nu^{(p)}(\vec{\kappa}; \omega)\sigma_{\vec{\kappa}\vec{\kappa}'} + n_0\sigma \times \sum_\lambda \chi^{(p)}_{\nu\lambda}(\vec{\kappa}; \omega)\chi_\lambda(\vec{\kappa}\vec{\kappa}\,'; \omega) + \sum_{\vec{l}''\lambda} \chi^{(p)}_{\nu\lambda}(\vec{\kappa}; \omega) \sum_{\vec{\kappa}''} e^{-i(\vec{\kappa}-\vec{\kappa}'')\cdot\vec{l}''} \times v_{\vec{l}''}\, \chi_\lambda(\vec{\kappa}''\vec{\kappa}\,'; \omega). \tag{33}$$

We rearrange this equation by transferring the second term to the left-hand side to obtain

$$\chi_\nu(\vec{\kappa}\vec{\kappa}\,'; \omega) = \tilde{\chi}^{(p)}(\vec{\kappa}; \omega)\delta_{\vec{\kappa}\vec{\kappa}'} \times \sum_{\vec{l}''\lambda} \tilde{\chi}^{(p)}_{\nu\lambda}(\vec{\kappa}; \omega) \sum_{\vec{\kappa}''} e^{-i(\vec{\kappa}-\vec{\kappa}'')\cdot\vec{l}''} \times v_{\vec{l}''}\, \chi_\lambda(\vec{\kappa}''\vec{\kappa}\,'; \omega), \tag{34}$$

where

$$\tilde{\chi}^{(p)}_\nu(\vec{\kappa}; \omega) = \sum_\lambda [\delta_{\nu\lambda} - n_0\sigma\chi^{(p)}_{\nu\lambda}(\vec{\kappa}; \omega)]^{-1} \times \chi^{(p)}_\lambda(\vec{k}; \omega), \tag{35}$$

and

$$\tilde{\chi}^{(p)}_{\nu\mu}(\vec{\kappa}; \omega) = \sum_\lambda [\delta_{\nu\lambda} - n_0\sigma\chi^{(p)}_{\nu\lambda}(\vec{\kappa}; \omega)]^{-1} \times \chi^{(p)}_{\lambda\mu}(\vec{\kappa}; \omega). \tag{35}$$

Transforming Eq. (3.4) back to real space, we get

$$\chi_\nu(\vec{l}\vec{l}\,'; \omega) = \tilde{\chi}^{(p)}_\nu(\vec{l} - \vec{l}\,'; \omega) + \sum_{l\mu} \tilde{\chi}^{(p)}_{\nu\mu}(\vec{l} - \vec{l}''; \omega)\chi_\mu(\vec{l}''\vec{l}\,'; \omega) v_{\vec{l}''}. \tag{36}$$

We now discuss how σ is to be chosen. While Eq. (36) is still exact and depends in detail upon the configuration of host and impurity sites, we go over directly to an effective medium by allowing $v_{\vec{l}''}$ to be zero, which corresponds to having only the coherent potential σ at each site $\vec{l}''$. The Green's function for this effective medium is simply $\tilde{\chi}^{(p)}_\nu(\vec{l} - \vec{l}\,'; \omega)$. We now consider a single impurity embedded in this effective medium. We note from Eq. (36) that the Green's function χ^{IM} describing this system satisfies

$$\chi^{IM}_\nu(\vec{l}\,\vec{l}\,'; \omega) = \tilde{\chi}^{(p)}_\nu(\vec{l} - \vec{l}\,'; \omega) + \sum_\mu \tilde{\chi}^{(p)}_{\nu\mu}(\vec{l}; \omega)\chi^{IM}_\mu(0\vec{l}\,'; \omega) v_I. \tag{37}$$

If we consider a single host atom embedded in the effective medium, we get a similar equation for the Green's function χ^H with v_I replaced by v_H. The CPA prescription for determining σ is that the single-site configuration average of the exact Green's function χ be equal to the effective medium Green's function:

$$c\chi^{IM}_\nu(\vec{l}\vec{l}\,'; \omega) + (1 - c)\chi^{(H)}_\nu(\vec{l}\vec{l}\,'; \omega) = \tilde{\chi}^{(p)}_\nu(\vec{l}\vec{l}\,'; \omega) \tag{38}$$

or equivalently,

$$c v_I \sum_\mu \tilde{\chi}^{(p)}_{\nu\mu}(l; \omega)\chi^{IM}_\mu(0\vec{l}\,'\omega) + (1 - c)v_H \sum_\mu \tilde{\chi}^{(p)}_{\nu\mu}(\vec{l}; \omega)\chi^H_\mu(0\vec{l}\,'; \omega) = 0. \tag{39}$$

We now solve for $\chi^{IM}(0\vec{l}\,'; \omega)$ from Eq. (37) by noting that $\tilde{\chi}^{(p)}_{\nu\mu}(\vec{l} = 0; \omega)$ is diagonal in the components ν and μ as pointed out previously. Obtaining $\chi^H(0\vec{l}\,'; \omega)$ in a similar fashion, we substitute these quantities into Eq. (39) to get

$$\frac{c(v - \sigma)}{1 - (v - \sigma)\tilde{\chi}^{(p)}_{\mu\mu}(0; \omega)} + \frac{(1 - c)(-\sigma)}{1 + \sigma\tilde{\chi}^{(p)}_{\mu\mu}(0; \omega)} = 0. \tag{40}$$

We observe that the quantity $\tilde{\chi}^{(p)}_{\mu\mu}(0; \omega)$ itself depends on σ through the relation

$$\tilde{\chi}^{(p)}_{\mu\mu}(0;\omega) = \sum_{\vec{\kappa}} \frac{\chi^{(p)}_{\mu\mu}(\vec{\kappa}; \omega)}{1 - (n_0\sigma/\kappa^2)\chi^{(p)}(\vec{\kappa}; \omega)}. \tag{41}$$

Equations (40) and (41) represent the principal result of this section, which enable us to solve for the coherent potential σ.

Having determined σ we obtain an expression for $\tilde{\chi}^{(p)}(\vec{\kappa},\omega)$, the average Green's function in the CPA, from Eq. (35a),

$$\tilde{\chi}^{(p)}(\vec{\kappa};\omega)=\frac{\chi_0(\vec{\kappa};\omega)}{1-[V_c(\vec{\kappa})+n_0\sigma/\kappa^2]\chi_0(\vec{\kappa};\omega)}\,. \tag{42}$$

Here we have expressed $\chi^{(p)}(\vec{\kappa};\omega)$ in terms of the bare electron-hole propagator as described in Sec. II. Note that the virtual-crystal approximation discussed in Sec. II is obtained from Eq. (42) by replacing σ by cv.

In addition to the electron density propagator given by Eq. (42), and the coherent potential σ, which is obtained by solving Eq. (40), we also require the $D^{IM}(\vec{\mathrm{l}}\,\mu,\vec{\mathrm{l}}\,\mu';\omega)$, the impurity displacement Green's function for a single impurity embedded in the medium of coherent potentials. This term will be used to describe light-scattering effects which are essentially due to individual scattering sites.

When one carries out the same calculations for $D(\vec{\mathrm{l}}\,\mu,\vec{\mathrm{l}}'\mu';\omega)$ starting from Eq. (22) that were presented for $\chi_\nu(\vec{\mathrm{l}}\vec{\mathrm{l}}';\omega)$, one finds

$$D^{IM}(0\mu,0\mu';\omega)=\delta_{\mu\mu'}D_0(\omega)\frac{1-\sigma\tilde{\chi}^{(p)}_{\mu\mu}(0;\omega)}{1-(v-\sigma)\tilde{\chi}_{\mu\mu}(0;\omega)}\,. \tag{43}$$

It is trivial to show that for $c\to 0$ this result reduces to the Sham-Maradudin propagator already derived as a special case.

Having now presented an approximation scheme that enables us to solve for the relevant Green's functions describing the impurity-electron system, we now turn to a description of light scattering as a probe of the system.

III. LIGHT-SCATTERING SPECTRA FOR THE SYSTEM

In this section, we turn to an analysis of the spectrum of light scattered inelastically from the model system. We shall see that a number of important features of the dynamics may be probed by such an experiment. The intensity of Raman scattering per unit solid angle in the frequency range from ω_s to $\omega_s+d\omega_s$ is

$$I(\omega_s)d\omega_s=\frac{\omega_i^4}{2\pi c^3}\sum_{\alpha\gamma}\sum_{\beta\lambda}n_\alpha n_\beta i_{\alpha\gamma,\beta\lambda}(\omega)E^-_\gamma E^+_\lambda d\omega_s, \tag{44}$$

where ω_i is the frequency of incident light, $\omega=\omega_i-\omega_s$ is the shift in the frequency of light on scattering, $\hat{n}$ is a unit vector describing the polarization of the scattered light and $\vec{\mathrm{E}}^+$ and $\vec{\mathrm{E}}^-[=(E^+)^*]$ are the amplitudes of the positive and negative frequency components of the incident light. The tensor $i_{\alpha\gamma,\beta\lambda}(\omega)$ is

$$i_{\alpha\gamma,\beta\lambda}(\omega)=\frac{1}{2\pi}\int_{-\infty}^{\infty}dt\,e^{i\omega t}\times\int\int d^3x\,d^3x'\times e^{-i\vec{\mathrm{q}}\cdot(\vec{\mathrm{x}}-\vec{\mathrm{x}}')}\langle\delta\chi_{\beta\lambda}(\vec{\mathrm{x}}t)\,\delta\chi_{\alpha\gamma}(\vec{\mathrm{x}}'0)\rangle\,, \tag{45}$$

where $\delta\chi_{\alpha\beta}(\vec{\mathrm{x}})$ is the change in the electronic contribution to the dielectric susceptibility of the crystal at the point $\vec{\mathrm{x}}$ produced by the excitations of interest. The wave vector $\vec{\mathrm{q}}=\vec{\kappa}_i-\vec{\kappa}_s$ is the difference between the incident and scattered wave vectors.

We take the fluctuating part of the dielectric susceptibility for the system we have described to have the form

$$\delta\chi_{\alpha\gamma}(\vec{\mathrm{x}})=n_0\sum_{\vec{\mathrm{l}}\mu}\delta(\vec{\mathrm{x}}-\vec{\mathrm{x}}(\vec{\mathrm{l}}))\,[c(\vec{\mathrm{l}})P_{\alpha\gamma,\mu}(\vec{\mathrm{l}})u_\mu(\vec{\mathrm{l}})+b_{\alpha\gamma,\mu}(\vec{\mathrm{l}})E^M_\mu(\vec{\mathrm{l}})]+\delta_{\alpha\gamma}\frac{\partial\chi}{\partial n}\delta n(\vec{\mathrm{x}}). \tag{46}$$

Here $P_{\alpha\gamma,\mu}(\vec{\mathrm{l}})$ is the first derivative of the electronic polarizibility with respect to the displacement amplitude $u_\mu(\vec{\mathrm{l}})$, and $b_{\alpha\gamma,\mu}(\vec{\mathrm{l}})$ is an electro-optical coefficient. For simplicity, we do not differentiate between host and impurity electro-optical coefficients. $E^M_\mu(\vec{\mathrm{l}})$ is the macroscopic electric field at the site $\vec{\mathrm{l}}$, which is given by

$$\vec{\mathrm{E}}^M(\vec{\mathrm{x}},t)=\vec{\mathrm{E}}_e(\vec{\mathrm{x}},t)+\vec{\mathrm{E}}_I(\vec{\mathrm{x}},t)\,,$$

where $\vec{\mathrm{E}}_e$ and $\vec{\mathrm{E}}_I$ are the induced fields from the electron gas fluctuations and impurity displacements, respectively.

Coulomb's law provides directly an expression for the electric field due to the electron density fluctuations

$$E_e(\vec{\mathrm{x}},t)=\frac{4\pi ie}{\epsilon_\infty}\sum_{\vec{\mathrm{Q}}}\frac{\vec{\mathrm{Q}}}{Q^2}\int d^3x\,e^{i\vec{\mathrm{Q}}\cdot(\vec{\mathrm{x}}-\vec{\mathrm{x}}')}\,\delta n(\vec{\mathrm{x}}',t)\,. \tag{47}$$

To compute the contribution to the macroscopic field from the impurities we use the Hertz vector, $\vec{\mathrm{Z}}(\vec{\mathrm{x}},t)$, which for our system satisfies

$$\nabla^2\vec{\mathrm{Z}}(\vec{\mathrm{x}},t)-\frac{\epsilon_\infty}{c^2}\frac{\partial^2\vec{\mathrm{Z}}}{\partial t^2}(\vec{\mathrm{x}},t)=-\frac{4\pi}{\epsilon_\infty}\vec{\mathrm{P}}_I(\vec{\mathrm{x}},t)\,, \tag{48}$$

where the impurity polarization density at $\vec{\mathrm{x}}$ and t is

$$\vec{\mathrm{P}}_I(\vec{\mathrm{x}},t)=-e^*\sum_{\vec{\mathrm{l}}}c(\vec{\mathrm{l}})\,\vec{\mathrm{u}}(\vec{\mathrm{l}}t)\delta(\vec{\mathrm{x}}-\vec{\mathrm{x}}(\vec{\mathrm{l}}))\,. \tag{49}$$

The solution to Eq. (48) is

$$\vec{\mathrm{Z}}(\vec{\mathrm{x}},t)=\frac{1}{\epsilon_\infty}\int d^3x'\,dt'\,\frac{\delta(t'+1/c\,|\vec{\mathrm{x}}-\vec{\mathrm{x}}'|-t)}{|\vec{\mathrm{x}}-\vec{\mathrm{x}}'|}\,\vec{\mathrm{P}}_I(\vec{\mathrm{x}}',t')$$

from which we obtain the field due to the impurities according to

$$\vec{E}_I(\vec{x},t) = \nabla[\nabla\cdot\vec{Z}(\vec{x},t)] - \frac{1}{c^2}\frac{\partial^2}{\partial t^2}\vec{Z}(\vec{x},t). \tag{50}$$

We require the field at lattice site $\vec{l}$ due to all impurities except the one that may exist at site $\vec{l}$. Thus, from Eqs. (49) and (50) we obtain

$$E_{I\mu}(\vec{x}(\vec{l}),t) = \frac{4\pi e^*}{\epsilon_\infty}\sum_{\vec{l}'\neq\vec{l}}\sum_{Q}\sum_{\mu'}(\hat{Q}_\mu\hat{Q}_{\mu'} - \delta_{\mu\mu'}) \times e^{i\vec{Q}\cdot(\vec{l}-\vec{l}')}c(\vec{l}')u_{\mu'}(\vec{l}'t), \tag{51}$$

where μ and μ' are Cartesian component indices and $\hat{Q} = \vec{Q}/|\vec{Q}|$, where the propagation effects (retardation effects) have been safely ignored for our purposes.

With the above expressions for the electric field we now express the electronic susceptibility fluctuation in terms of the impurity displacements and the electron density deviation:

$$\begin{aligned}\delta\chi_{\alpha\beta}(\vec{x}t) = \frac{1}{n}\Bigg[&\sum_{\vec{l}\mu}\delta(\vec{x}-\vec{x}(\vec{l}))c(\vec{l})P_{\alpha\gamma,\mu}u_\mu(\vec{l}t) + \sum_{\vec{l}\mu}\delta(\vec{x}-\vec{x}(\vec{l}))b_{\alpha\gamma,\mu}\left(\frac{4\pi ie}{\epsilon_\infty}\right)\sum_{\vec{Q}}\frac{\hat{Q}_\mu}{|\vec{Q}|}\int d^3x'' e^{i\vec{Q}\cdot(\vec{x}-\vec{x}'')}\delta n(\vec{x}''t)\\ &+\sum_{\vec{l}\mu}\delta(\vec{x}-\vec{x}(\vec{l}))b_{\alpha\gamma,\mu}\left(\frac{4\pi e^*}{\epsilon_\infty}\right)\sum_{\vec{l}''\neq\vec{l}}c(\vec{l}'')\sum_{\vec{Q}}\sum_{\nu}(\hat{Q}_\mu\hat{Q}_\nu - \delta_{\mu\nu})e^{i\vec{Q}\cdot(\vec{l}-\vec{l}')}u_\nu(\vec{l}''t)\Bigg]\\ &+\delta_{\alpha\gamma}\frac{\partial\chi}{\partial n}\delta n(\vec{x}t).\end{aligned} \tag{52}$$

Thus, we can express the Raman scattering intensity, which from Eq. (45) depends on the susceptibility-susceptibility correlations, in terms of correlations between electron density fluctuations and impurity ion displacements. Specifically when the expressions are written out in full, we encounter four correlation functions $\langle\delta n(\vec{x}t)\delta n(\vec{x}'0)\rangle$, $\langle\vec{u}(\vec{l}t)\vec{u}(\vec{l}'0)\rangle$, $\langle\delta n(\vec{x}t)\vec{u}_\mu(\vec{l}',0)\rangle$, and $\langle\vec{u}_\mu(\vec{l}t)\delta n(\vec{x}'0)\rangle$. These are each related to their corresponding retarded Green's functions according to

$$\langle A(t)B(0)\rangle = \frac{1}{2}\int d\omega\, e^{-\omega t}[n(\omega)+1]\mathrm{Im}G^R_{AB}(\omega),$$

where $n(\omega) = (e^{\beta\omega}-1)^{-1}$. $G^R_{AB}(\omega)$ is the Fourier transform of $G^R_{AB}(t)$, which is defined by

$$G^R_{AB}(t) = -i\Theta(t)\langle[A(t),B(0)]\rangle. \tag{53}$$

Each of the retarded Green's functions which we require can be related to the Green's functions presented in Sec. II. For example, starting with

$$\vec{G}^R_{\vec{l}\vec{x}'}(t) = -i\Theta(t)\langle[\vec{u}(\vec{l}t), \delta n(\vec{x}'0)]\rangle,$$

we obtain after two time differentiations, application of the equations of motion, and transforming the time variable

$$\vec{G}^R_{\vec{l}\vec{x}'}(\omega) = \frac{D_0(\omega)\gamma_0 c(l)}{(2m_l\omega_0)^{1/2}}\sum_{\vec{q}}\frac{\vec{q}}{q^2}e^{i\vec{q}\cdot(\vec{x}'-\vec{l})}\chi^R(-\vec{q},\omega). \tag{54}$$

The other retarded Green's functions can be related to χ^R in the same fashion. In addition, a formal identity between the retarded Green's function, and the imaginary time Green's function studied in the previous sections enables us to write

$$\chi^R(\vec{q},\omega) = \mathrm{Re}\chi(\vec{q},\omega+i\eta) + (\mathrm{sgn}\omega)\,\mathrm{Im}\chi(\vec{q},\omega+i\eta).$$

We express each of the correlation functions in terms of the effective medium Green's functions we solved for in Sec. II, and find

$$\langle\delta n(\vec{x}t)\delta n(\vec{x}'0)\rangle = -2\int d\omega\, e^{-i\omega t}[n(\omega)+1]\sum_{\vec{\kappa}}e^{i\vec{\kappa}\cdot(\vec{x}-\vec{x}')}[\mathrm{Im}\chi^R(\vec{\kappa},\omega^+)] \tag{55a}$$

$$\langle u_\mu(\vec{l}t)\delta n(\vec{x}'0)\rangle = -\frac{2\gamma_0 c(\vec{l})}{(2M_l\omega_0)^{1/2}}\sum_{\vec{\kappa}}\frac{\kappa_\mu}{\kappa^2}e^{i\vec{\kappa}\cdot(\vec{x}'-\vec{l})}\int d\omega\, e^{-i\omega t}[n(\omega)+1][\mathrm{Im}D^0(\omega^+)\chi(-\vec{q},\omega^+)], \tag{55b}$$

$$\langle\delta n(\vec{x}t)u_{\mu'}(\vec{l}'0)\rangle = -\frac{2\gamma_0 c(\vec{l})}{(2M_l\omega_0)^{1/2}}\sum_{\vec{\kappa}}\frac{\kappa_{\mu'}}{\kappa^2}e^{i\vec{\kappa}\cdot(\vec{x}-\vec{l}')}\int d\omega\, e^{i\omega t}[n(\omega)+1][\mathrm{Im}D^0(\omega^+)\chi(\vec{q},\omega^+)] \tag{55c}$$

$$\begin{aligned}\langle u_\mu(\vec{l}t)u_{\mu'}(\vec{l}'0)\rangle = &-\frac{\delta_{\vec{l}\vec{l}'}\delta_{\mu\mu'}}{M_l\omega_0}c(\vec{l})\int d\omega\, e^{-i\omega t}[n(\omega)+1][\mathrm{Im}D^0(\omega^+)]\\ &+\frac{\gamma_0^2 c(\vec{l})c(\vec{l}')}{M_l\omega_0}\sum_{\vec{\kappa}}\frac{\kappa_\mu\kappa_{\mu'}}{\kappa^4}e^{i\vec{\kappa}\cdot(\vec{l}-\vec{l}')}\int d\omega\, e^{-i\omega t}[n(\omega)+1][\mathrm{Im}D^0(\omega^+)\chi(\vec{\kappa},\omega^+)].\end{aligned} \tag{55d}$$

TABLE I. Numerical values of parameters used in computations.

High-frequency dielectric constant ϵ_∞	10.9 (Ref. 16)
Electron effective mass m^*	$0.0775 m_0$
Ion effective charge e^*	$2.0e$ (Ref. 17)
Local-mode phonon frequency ω_0	350 cm^{-1}
Electro-optical coefficient $\lvert b \rvert$	8.4×10^{-7} esu/dyn (Ref. 18)
Elasto-optical coefficient $\lvert P \rvert (P\times b/\lvert P\times b\rvert = -1)$	6.4×10^{7} cm^{-1} (Ref. 18)
Damping of local-mode phonon γ	$0.03\times\omega_0$
Electron density n	1.1×10^{18} cm^{-3}
Classical electron-plasma frequency $(4\pi n e^2/\epsilon_\infty m^*)^{1/2}$	347 cm^{-1}
Impurity concentration c	0.05
Temperature T	300 °K
Incident wavelength	6228 Å
Refractive index n_i	3.78 (Ref. 19)

Here $\omega^+ = \omega + i\eta$.

By choosing the effective medium approximation for χ as given by Eq. (42), one can obtain a general form for the Raman-scattering intensity by using the above expressions for the correlation functions that contribute to $\langle\delta\chi\delta\chi\rangle$ in Eq. (45). This is the procedure we follow with one qualification: The auto correlations at a given site $\vec{1}$, should reduce to the single-impurity limit when the impurity concentration goes to zero. We build this limit into our description of the Raman scattering by expressing $\langle u_\mu(\vec{1}t)u_{\mu'}(\vec{1}0)\rangle$, the diagonal impurity correlation function, in terms of the Green's function given by Eq. (23). This is the impurity Green's function for a real impurity embedded in the effective medium of coherent potentials. We thus have

$$\langle u_\mu(\vec{1}t)u_{\mu'}(\vec{1}0)\rangle = -\frac{\delta_{\mu\mu'}c(\vec{1})}{M_i\omega_0}\int d\omega\, e^{-i\omega t}[n(\omega)+1]\left\{\text{Im}D^0(\omega^+)\left(\frac{1-\sigma\tilde{\chi}^{(p)}_{\mu\mu}(0;\omega)}{1-(v-\sigma)\tilde{\chi}^{(p)}_{\mu\mu}(0;\omega)}\right)\right\} . \tag{56}$$

Rather than present the general expression for the Raman-scattering efficiency, we restrict our attention in what follows to a few special geometries, each of which illustrates different aspects of the scattering processes. Our computations are based on numbers appropriate to $\text{GaAs}_{1-x}P_x$, and we choose parameters appropriate to GaAs as shown in Table I. For simplicity the phosphorus is taken to represent only an isotopic impurity in the host lattice. The single parameter that could depend strongly on whether the lattice site is a host or impurity is the ion effective charge, and its value in the literature is the same for both GaP and GaAs.[17]

All CPA computations required first an evaluation of $\sigma(\omega)$ from Eq. (40). Using the numerical values of the parameters as displayed in Table I, we find that $\sigma(\omega)$ is remarkably close to the virtual-crystal approximation over the entire frequency and composition range of interest here. The deviation was less than 1% for $|\omega-\omega_0|/\omega_0 < 0.001$, and much less for frequencies away form ω_0. Basically, this is a consequence of the long wavelength of the plasma excitation compared to the typical impurity spacing. Clearly, at 5% impurity concentration, the value used in our computations, and at wave vectors appropriate to the light-scattering experiment, the system is well described as a uniform effective medium, and, as displayed below, the predominant features in the spectrum are the collective excitations of the system.

In all computations the Lindhard expression[14] for the real part of $\chi_0(q,\omega)$ was taken, while the exact expression for the imaginary part was used.[15] In this way the finite wave-vector behavior of the electron gas, including the breakup of the plasmon into single particle excitations, is built into the computations.

We now turn to an analysis of these specific geometries.

(a) In this case $\vec{E}_i$ and $\vec{E}_s$, the incident and scattered electric fields, respectively, are parallel and along a principal axis of the crystal. Only a single term contributes to the scattering efficiency. This follows from utilizing the relations $P_{\alpha\beta\gamma} = P|\epsilon_{\alpha\beta\gamma}|$ and $b_{\alpha\beta\gamma} = b|\epsilon_{\alpha\beta\gamma}|$, where $\epsilon_{\alpha\beta\gamma}$ is the Levi-Civita tensor, appropriate for crystals of the zinc-blende structure, and we find

$$I^{(a)}(\omega_s)d\omega_s = \frac{\omega_i^4}{\pi c^3}\left(\frac{\partial\chi}{\partial n}\right)^2 |E|^2[n(\omega)+1][\text{Im}\chi(q,\omega^+)]d\omega_s . \tag{57}$$

In Fig. 2 is a plot of the frequency dependence of $I^{(a)}(\omega_s)d\omega_s$ for several values of κ, the dimensionless wave vector defined by $\kappa = \hbar q/(2m^*k_BT)^{1/2}$. κ in turn can be related to the scattering angle, θ, from the kinematic restriction

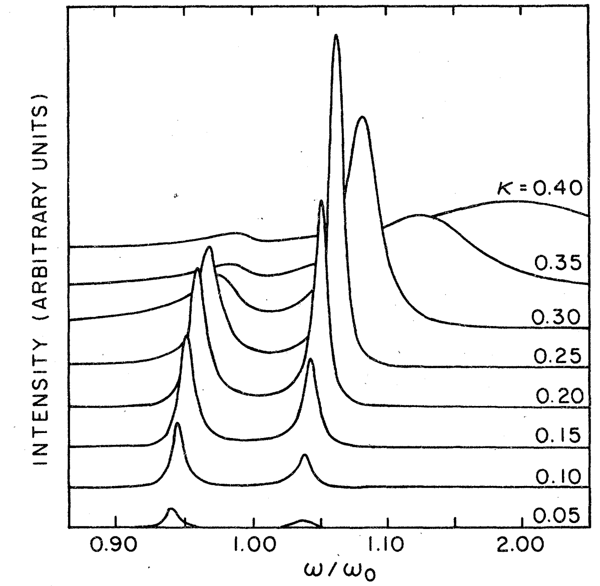

FIG. 2. Frequency variation of the Raman scattering intensity for several values of κ, the dimensionless wave-vector transfer defined by $\kappa = |\vec{q}_s - \vec{q}_i|(\hbar^2/2m^* k_B T)^{1/2}$, for geometry (a) described in the text, and parameters listed in Table I.

$$c^2 q^2 = n_i^2 \omega_i^2 + n_s^2 \omega_s^2 - 2 n_i n_s \omega_i \omega_s \cos\theta \,, \tag{58}$$

where n_i and n_s are the refractive indices at the incident and scattered frequencies, respectively. For example, for the 6228 Å He-Ne line one finds the relation between κ and θ as shown in Fig. 3. Since the frequency shift is small, we have expanded the refractive index about its value at the incident frequency and plotted the angular dependence of the average value of $\kappa(\omega)$.

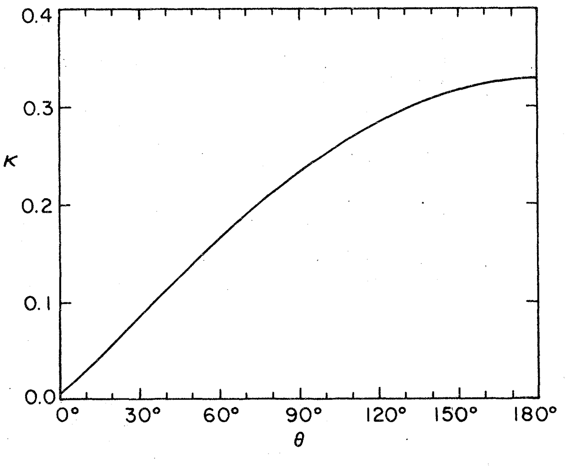

FIG. 3. Relation of κ to the scattering angle, for the 6328-Å He-Ne line.

From Fig. 3 we note that κ takes on a maximum value of about 0.32 for backscattering, which in Fig. 2 corresponds to the region where the higher-frequency resonance begins to become heavily damped. This is strictly an effect of the electron gas and is due to the Landau damping of the plasmon contribution to the collective mode. In fact, within the range of attainable wave vectors one notes the presence of two modes which occur at approximately

$$\omega_\pm(q) = \tfrac{1}{2}[\omega_s + \omega_p(q)] \pm \tfrac{1}{2}\Big\{[\omega_s + \omega_p(q)]^2 - 4c\,\omega_p^2(q)\,\Omega_p^2(m_L/m_i)\Big\}^{1/2} . \tag{59}$$

This expression is obtained from Eq. (42) by taking the small $\vec{q}$ limit

$$\chi_0(\vec{q} \to 0, \omega) = (n_e/m^*)(q^2/\omega^2) .$$

In Eq. (59), $\omega_p(q)$ is given by

$$\omega_p(q \to 0) = (4\pi n e^2/\epsilon_\infty m^*)^{1/2}\left[1 + \tfrac{9}{10}(q/q_{\mathrm{TF}})^2\right] ,$$

where q_{TF} is the Thomas-Fermi wavenumber $q_{\mathrm{TF}} = (6\pi n e^2/\epsilon_{\mathrm{F}})^{1/2}$, with ϵ_{F} the Fermi energy $\epsilon_{\mathrm{F}} = (3\pi^2 n)^{2/3}/2m^*$. In obtaining the approximation given in Eq. (59) we have simply replaced σ with cv the virtual crystal effective potential.

(b) A particularly simple form for the Raman scattering efficiency results by taking $\vec{E}_i$ and $\vec{E}_s$ to be orthogonal and along principal axes of the crystal, while $\vec{q}$ lies in the plane defined by $\vec{E}_i$ and $\vec{E}_s$. Then one obtains simply

$$I^{(b)}(\omega_s)\,d\omega_s = -\frac{\omega_i^4}{\pi c^3}\,\frac{fP^2}{2m_i\omega_0 n}\,|E|^2[n(\omega)+1] \times \mathrm{Im}\,D^0(\omega^+)\left(\frac{1 - \sigma\tilde{\chi}_{\mu\mu}^{(p)}(0;\omega^+)}{1 - (v-\sigma)\tilde{\chi}_{\mu\mu}^{(p)}(0;\omega)}\right)d\omega_s \,. \tag{60}$$

Here we have denoted the impurity concentration by f and the speed of light by c.

The effective medium correction in Eq. (60) is very minor for the frequency range and impurity concentration chosen here, and one finds in Fig. 4 a single peak in the frequency dependence of the scattering efficiency at the nearly unshifted local mode frequency. The lack of coupled collective modes in this particular geometry is a consequence of the fact that it is the transverse local mode that produces this effect.

(c) If one chooses $\vec{E}_i$, $\vec{E}_s$, and $\vec{q}$ to be mutually perpendicular and to lie along the principal axes of the crystal the form of the scattering intensity is seen to be

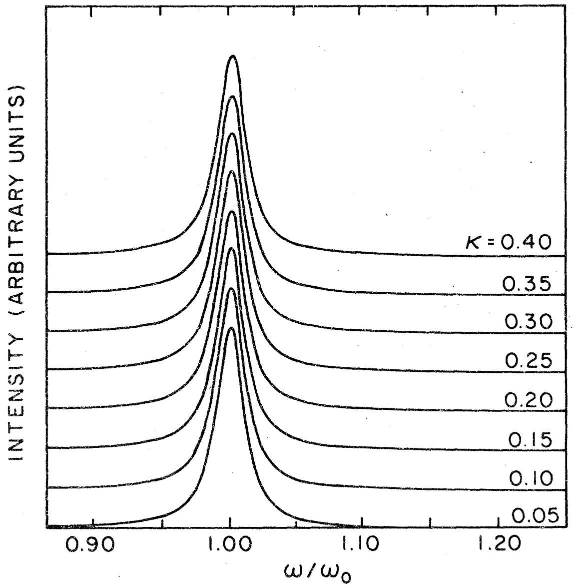

FIG. 4. Frequency variation of the Raman scattering intensity for several values of κ, for geometry (b) described in text.

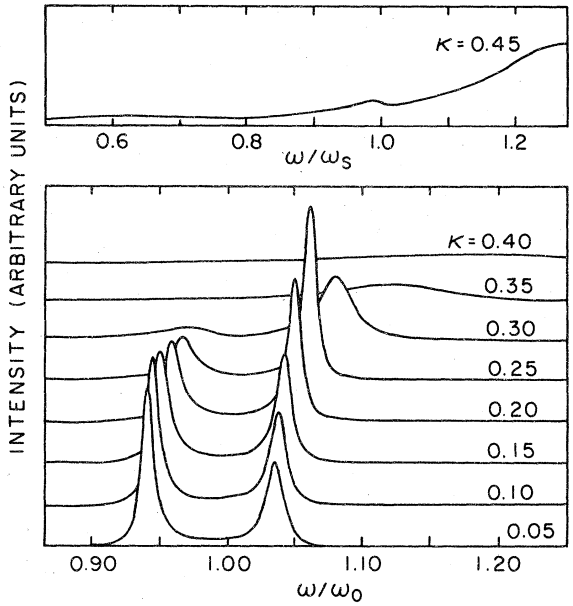

FIG. 5. Frequency variation of the Raman scattering intensity for several values of κ, for geometry (c) described in text. Top figure shows emergence of nearly unshifted local-mode peak at longer wave-vector transfers.

$$
\begin{aligned}
I^{(c)}(\omega_s)d\omega_s = {} & I^{(b)}(\omega_s)d\omega_s + \frac{\omega_l^4}{\pi c^3}\,\frac{\gamma_0^2 f^2}{2m_l\omega_0}P^2\,|E\,|^2[n(\omega)+1]\frac{1}{q^2}[\mathrm{Im}D_0^2(\omega^+)\chi(q,\omega^+)]d\omega_s \\
& - \frac{2\omega_l^4}{\pi c^3}\,\frac{\gamma_0 f}{(2m_l\omega_0)^{1/2}}Pb\left(\frac{4\pi i e}{\epsilon_\infty}\right)|E\,|^2[n(\omega)+1]\frac{1}{q^2}[\mathrm{Im}D_0(\omega^+)\chi(q,\omega^+)]d\omega_s \\
& - \frac{\omega_l^4}{\pi c^3}\left(\frac{4\pi e^2}{\epsilon_\infty}\right)^2 b^2\,|E\,|^2[n(\omega)+1]\frac{1}{q^2}[\mathrm{Im}\chi(q,\omega^+)]d\omega_s\,.
\end{aligned}
\tag{61}
$$

The frequency dependence of the scattering efficiency for this case is shown in Fig. 5. Here one sees evidence of both the coupled modes, and the incoherent scattering of the transverse local modes. The latter effect is much weaker, however, and is noticeable only for fairly large values of $\vec{q}$. It may be that this unshifted uncoupled mode can be probed in this geometry by choosing different impurity and electron concentrations or another incident frequency.

Summarizing the results of our computations, we see that the inelastic scattering of light by the system we have described provides a means of detecting both collective excitations due to the coupling of the local modes to the electron gas, and the nearly unshifted transverse excitation that was the subject of the work of Sham and Maradudin.

ACKNOWLEDGMENT

This work was supported in part by AFOSR OAR Grant No. 77-2887.

---

[1] A. Mooradian and A. L. McWhorter, in *Light Scattering Spectra of Solids*, edited by G. B. Wright (Springer-Verlag, New York, 1969), p. 297

[2] L. J. Sham and A. A. Maradudin, Solid State Commun. 5, 337 (1967).

[3] W. G. Spitzer (private communication).

[4] B. Velicky, S. Kirkpatrick, and H. Ehrenreich, Phys. Rev. 175, 747 (1968).

[5] A. A. Maradudin and J. Oitmaa, Solid State Commun. 1, 1143 (1969).

[6] D. L. Mills and A. A. Maradudin, Phys. Rev. B 1, 903 (1970).

[7] In the one-impurity limit, our results are in fact more complete than those of Sham and Maradudin, in that we find complete expressions for the relevant response functions. They discuss only the frequency shift produced by the plasmon local-mode interaction.

[8] A. A. Abrikosov, L. P. Gorkov, and I. Ye. Dzyaloshin-

ski, *Quantum Field Theoretical Methods in Statistical Mechanics* (Pergamon, New York, 1965).

[9] R. J. Elliott, J. A. Krumhausl, and P. L. Leath, Rev. Mod. Phys. **46**, 465 (1974).

[10] D. W. Taylor, Phys. Rev. **156**, 1017 (1967).

[11] Our equations are also isomorphic to those which describe the vibrations of a lattice of two isotopes distributed randomly. See D. W. Taylor, Ref. 10.

[12] See D. L. Mills, M. T. Béal-Monod and P. Lederer, in *Magnetism*, edited by H. Suhl (Academic, New York, 1973) Vol. 5, p. 28.

[13] J. A. Harrington and R. Weber, Solid State Commun. **11**, 1435 (1972).

[14] J. Lindhard, K. Dan. Vidensk. Selsk. Mat. Fys. Medd. **28**, 408 (1954).

[15] R. Sirko and D. L. Mills, Phys. Rev. B (to be published).

[16] M. Haas and B. W. Herris, J. Phys. Chem. Solids **23**, 1099 (1965).

[17] S. Ushioda, Ph.D. thesis (University of Pennsylvania, 1969) (unpublished).

[18] A. Mooradian and A. L. McWhorter, Phys. Rev. Lett. **19**, 849 (1967).

[19] See *Semiconductors and Semimetals*, edited by R. K. Willardson and A. C. Beer (Academic, New York, 1967), Vol. 3, p. 519.